International Journal of Chemical Science
Online ISSN: 2523-2843, Print ISSN: 2523-6075; Impact Factor: RJIF 5.22
Received: 21-11-2018; Accepted: 25-12-2018
www.chemicaljournals.com
Volume 3; Issue 1; January 2019; Page No. 30-37

Regulating localized corrosion rate of acidified ASTM A36 mild steel with *Oenothera biennis* extracts using thermometric and potentiodynamic polarization studies

Benedict U Ugi[1*], Thomas O Magu[2]
[1] Department of Pure and Applied Chemistry, University of Calabar, PMB, Calabar, Nigeria
[2] CAS Key Laboratory of Green Printing, Institute of Chemistry, Chinese Academy of Sciences, Beijing, PR China

Abstract
Regulating localized corrosion rate of acidified ASTM A36 mild steel with *Oenothera biennis* extracts was carried out using thermometric and Potentiodynamic polarization as experimental techniques. Various parameters of measurements adopted in this study included but not limited to enthalpy of adsorption, entropy of adsorption, Gibbs free energy of adsorption, adsorption parameters, activation energy, collision coefficient, corrosion current density, corrosion potential, inhibition efficiency, cathodic and anodic slope values etc. Results from the research showed that both alkaloid and flavonoid extracts of *Oenothera biennis* flowers (AEOBF and FEOBF) acted as reliable corrosion inhibitors for ASTM A36 mild steel in HCl medium with inhibition efficiency of 97.6 and 91.4% respectively at lower temperature (303 K) and also at moderately higher temperatures (313 and 323 K). Result from both experiments were in agreement as values for inhibition efficiency for AEOBF were higher compared to those of FEOBF indicating that the adsorption of the alkaloid fraction was stronger than flavonoids. The mechanism of action was physical and the adsorption process was monolayer. Both inhibitors showed very stabled, endothermic, spontaneous and associative reaction process on the ASTM A36 mild steel which made desorption upon agitation at moderate temperatures quite difficult.

Keywords: polarization, ASTM A36 mild steel, *Oenothera biennis*, hydrochloric acid, localized corrosion, heteroatoms, gamolenic acid, thermometric

1. Introduction
The consequences of corrosion especially localized corrosion (which is quite uneasy to detect at its early stage) on systems employing ASTM A36 as their major metal of construction cannot be over emphasized. Corrosion on its own is simply the deterioration of a material (especially metal) of its fundamental composition when exposed to its immediate environment. Corrosion issues are noticed with the construction industries, shipping companies, electrical industries, aviation industries and a whole lot of other areas [1-2]. Different approached to the possible control of corrosion impact on materials are available. The consequence of these approaches ranging from their environmental unfriendliness, toxicity, non-renewability, high cost of production etc. make them not really applicable. Sequel to that, organic inhibitors became an intense area of research not only because of their ability to overcome the drawbacks earlier highlighted but their ability to bind to metal surfaces due to the presence of hetero atoms (P, S, N, etc.) from the hetero compounds – alkaloids, flavonoids, saponins, tanins, etc. [1-3]. The use of corrosion inhibitors, mainly organic heterocyclic compounds, has been reported to be one of the most operational and functional approaches against corrosion, as these can easily interact and adsorb on metal surfaces via electron-rich centers constituted mainly of heteroatoms (P, O, S, N), p-electrons of multiple (double and triple) bonds and phenyl rings. ASTM A36 is the most commonly used mild and hot rolled steel. It has excellent welding properties and is suitable for grinding, punching and tapping, drilling and machining processes [3-4]. ASTM A36 is usually available in the following forms: Rectangle bar, Square bar, Circular rod, Steel shapes such as channels, angles, H beams and I beams. ASTM A36 steel has the following applications: bolted, riveted or welded construction of bridges, buildings and oil rigs. It is used in forming tanks, bins, bearing plates, fixtures, rings, templates, jigs, sprockets, cams, gears, base plates, forgings, ornamental works, stakes, brackets, automotive and agricultural equipment, frames, machinery parts. It is used for various parts obtained by flame cutting such as in parking garages, walkways, boat landing ramps and trenches [4]. ASTM A36 steel is easy to weld using any type of welding methods, and the welds and joints so formed are of excellent quality. The machinability rate of ASTM A36 is estimated to be 72%, and the average surface cutting feed of ASTM A36 is 120 ft/min. Fragrant and showy, *Oenothera biennis* (Common evening primrose) is an erect biennial featuring large, bowl-shaped, lemon-scented, yellow flowers, up to 2 in. across (5cm), at the top of a stiff, purple-tinged flower stem. Blooming profusely from early summer to early fall, the flowers open in the evening and remain open through late morning [5]. They rise on leafy, branched stems from a basal rosette of oblong, long medium green leaves. This evening primrose complete its life cycle in 2 years, its basal leaves becoming established the first year, while flowing occurs the second year. The whole plant is edible: the leaves can be cooked as green vegetables and the flowers make beautiful salad garnish. The major active compound in the *Oenothera biennis* plant is Gamma – linolenic (Gamolenic) acid ((6Z,9Z,12Z)-octadeca-6,9,12-trienoic acid) whose structure is shown in Fig. 1.

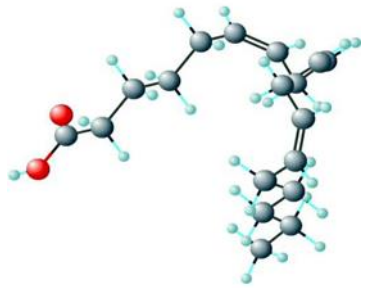

Fig 1: Gamma – linolenic (Gamolenic) acid ((6Z, 9Z, 12Z)-octadeca-6, 9, 12-trienoic acid). Major constituent in the oil of *Oenothera biennis*

Gamma-Linolenic acid (GLA) (18 carbon atoms), from the Latin linon, meaning flax, plus oleic, meaning oil or olive oil, was isolated from seed and flower oil of *Oenothera biennis* (evening primrose). The structure was first proposed by Eibner A. and Luft K. in 1927, and later confirmed by Riley J.P. in 1949. Gamma-Linolenic acid was synthesized in 1961 by Osbond J.M. *et al*. It is a polyunsaturated fatty acid (PUFA) with three cis (Z) double bounds (the first one from the methyl end is in n-6 or omega-6 (ω-6) so in shorthand 18:3n-6) member of the sub-group called long chain fatty acids (LCFA), from 14 to 18 carbon atoms [5].
Following the growing need for eco-friendly, non- toxic, renewable and cost effective corrosion inhibitors, research on regulating localized corrosion rate of acidified ASTM A36 mild steel with *Oenothera biennis* extracts using thermometric and potentio-dynamic polarization studies became important especially on the grounds that hetero-compounds of this plant has been extensively researched upon in pharmacology and food chemistry with limited or no work at all in the field of green corrosion chemistry [5].

2. Experimentation

2.1 ASTM A36 Mild Steel Composition and pre-preparation

Table 1 shows the chemical composition of ASTM A36 Mild Steel measured in percentage.

Table 1: Chemical Composition of ASTM A36 Mild Steel [5]

Element	Content
Carbon, C	0.25 – 0.29%
Copper, Cu	0.20%
Iron, Fe	98.0%
Manganese, Mn	1.03%
Phosphorous, P	0.040%

The sheet of ASTM A36 mild steel which was obtained from Engineering Department of Cross River University of Technology, Calabar – Nigeria was reshaped into multiple numbers of dimension of 3.5 cm x 0.05 cm by the Mechanical Engineering Department of the University for Thermometric Analysis and 1 cm x 1 cm for Potentiodynamic polarization studies. The various metals were then polished to mirror surface using different grades of silicon carbide paper, degreased in ethanol to remove the surface dirt arising from the abraded process, rinsed with acetone and air dried. The prepared metal substrates were stored in a desiccator prior to use.

2.2 Preparation of crude flower extracts

Oenothera biennis (evening primrose) flowers were washed and then dried in oven at 35^0 C, followed by grinding to obtain a powdered sample with very fine particle size. The powdered sample was extracted in methanol using hot extraction process. The mixture of flower extract and methanol (solvent) was removed from heat and placed in a water bath for 8 hours to evaporate the solvent leaving the crude flower extracts (paste).

2.3 Alkaloid and Flavonoids inhibitor preparation

Sixty five grams of the crude extract was partitioned between 100 ml 1 M HCl and chloroform respectively with the use of a separating funnel. Two non-homogenous mixture was obtained after rigorous shaking of the flask and which was later allowed to settle for 3 hours. The tailing solution which is the non-alkaloid was separated and discarded while the HCl solution in the float fraction from the separating funnel was carefully basify with 200 ml ammonia solution and this was taken well above pH 7. 100 ml of chloroform was immediately added into the basic solution in the separating funnel to obtain two immiscible layers with the lower one containing the alkaloids. The chloroform layer was eventually separated from mixture and put aside, the chloroform distilled off, and a small quantity of the crude alkaloids was obtained.
In another experiment, 100 g of the dried powdered sample was weighed into a beaker and extracted with 100 ml of ethanol at room temperature for 1 hour. The solution was filtered and the filtrate was evaporated to dryness over water bath at 50^0 C. The weight of the dried extract was taken and the amount of flavonoid present was calculated.
In preparing the stock solutions (inhibitors), 2 g each of both the crude flavonoids and alkaloids extracts were separately soaked in ½ litre of HCl solution and kept for 1 day. The solutions obtained were filtered and stored. From the stock solution, inhibitor test solution of concentrations 1.0 g/L, 3.0 g/L, 5.0 g/L, 7.0 g/L and 10.0 g/L was prepared. The prepared solutions were then used to study the corrosion inhibition impact of the phytochemical compounds.

2.4 Thermometric measurements

Hundred ml of the 1.5 M HCl solution was emptied into a beaker and ASTM A36 mild steel of dimension 3.5 cm x 0.05 cm already weighed was dropped into the beaker while the beaker was immediately immersed in a water bath. The volume of the hydrogen gas evolved from the corrosion reaction was regulated by temperature changes in the water bath. After every 1 hour at different temperatures of 303 K, 313 K and 323 K, the metal was removed, degreased with ethanol, rinsed with acetone and air dried and then weighed. This procedure was repeated for a set of fresh metals at different concentrations of 1.0 g/L, 3.0 g/L, 5.0 g/L, 7.0 g/L and 10.0 g/L for the inhibitors.

2.5 Potentiodynamic polarization studies

ASTM A36 mild steel of dimension 1 cm x 1 cm, graphite rod and silver/silver chloride (Ag/AgCl) were used as working, counter and reference electrodes, respectively for the Potentiodynamic polarization measurement using the Gamry electrochemical instrument framework. The potentiodynamic polarization curves were recorded from cathodic potential of -2.5 eV to anodic potential of +2.5 eV at a scan rate of 0.5 mV s^{-1} with respect to free corrosion potential (E_{corr}). The linear Tafel segments of the anodic and cathodic curves were extrapolated to corrosion potential to

obtain the corrosion current densities (icorr) and other electrochemical parameters of interest.

3. Result

3.1 Thermometric results (Temperature dependent)

The following mechanism can be proposed for hydrogen evolution reaction on electrodes in acidic media during thermometric experiment (Uwah *et al*. 2013, Okafor *et al*. 2007):

1. A primary discharge step (Volmer reaction):

$$M + H_3O^+ + e- \; MH_{ad} + H_2O$$

2. An electrochemical-desorption step (Heyrowsky reaction)

$$MH_{ad} + H_3O^+ + e- \; M + H_2 + H_2O$$

3. A recombination step (Tafel reaction):

$$MH_{ad} + MH_{ad} \; 2M + H_2$$

For hydrogen evolution reaction, the cathodic reaction may have three steps: first, water molecule or hydronium ion is discharged onto the electrode surface to produce hydrogen atom in acidic solution and adsorbed hydrogen atom, MH_{ad}. Second, one electron is transferred to a hydronium ion and the hydrogen evolution reaction occurs on metal surface (Heyrowsky reaction) or a pure chemical reaction takes place subsequently (Tafel reaction) [3, 6-7]. In spite of three states for the formulation of the mechanism, no one of the three reactions formulated occurs as a single step but combined with another. The results obtained however showed that the corrosion rate decrease with increase in concentrations of both inhibitors, but increased with increase in temperature (Table 2). From the corrosion rates, the inhibition efficiency was calculated and the result showed increases% IE with increase in inhibitor concentrations as well as decrease with increase temperature. This revealed that, fractions of *Oenothera biennis* extracts are adsorbed on the metal surface thereby protecting metal from the action of acid and the latter suggest a desorption phenomenon following weak forces of attraction due to high temperature effects. This is in agreement with the observation of other workers [8-10]. The trend in temperature suggests physical adsorption respectively.

Table 2: Thermometric experiment result for ASTM A36 mild steel in 1.5 M HCl solution in the presence of various concentrations of *AEOBF and FEOBF at different temperatures*

Inhibitors	Systems	Corrosion rate (mg/cm2/h)			Surface coverage			Inhibition efficiency (%)		
	Conc. (g/L)	303K	313K	323K	303K	313K	323K	303K	313K	323K
AEOBF	Blank (1.5 M HCl)	12.097	15.515	19.442	-	-	-	-	-	-
	1.0 g/L	5.000	8.090	15.744	0.587	0.479	0.190	58.7	47.9	19.0
	3.0 g/L	4.177	6.997	11.796	0.655	0.549	0.393	65.5	54.9	39.3
	5.0 g/L	3.016	4.713	9.793	0.751	0.696	0.496	75.1	69.6	49.6
	7.0 g/L	1.894	3.278	6.195	0.843	0.789	0.681	84.3	78.9	68.1
	10.0 g/L	0.286	1.542	3.847	0.976	0.901	0.802	97.6	90.1	80.2
FEOBF	Blank (1.5 M HCl)	12.097	15.515	19.442	-	-	-	-	-	-
	1.0 g/L	4.121	8.274	12.840	0.659	0.467	0.340	65.9	46.7	34.0
	3.0 g/L	2.759	6.488	10.576	0.772	0.582	0.456	77.2	58.2	45.6
	5.0 g/L	1.924	5.761	8.758	0.841	0.629	0.550	84.1	62.9	55.0
	7.0 g/L	1.709	3.101	5.727	0.859	0.800	0.705	85.9	80.0	70.5
	10.0 g/L	1.038	2.558	4.517	0.914	0.835	0.768	91.4	83.5	76.8

3.2 Potentiodynamic polarization studies of inhibitor/metal interaction

The anodic and cathodic polarization curves of ASTM A36 mild steel in 1.5 M HCl with and without the various concentrations of AEOBF and FEOBF are presented in Figure 2a - b. The Potentiodynamic polarization parameters (E_{corr}, I_{corr}, β_a and β_b) were obtained from the intersection of anodic and cathodic Tafel slopes of the polarization curves and this values are shown in Table 3 [8-11]. Table 4 show that both the cathodic and anodic curves showed lower current densities in the presence of the extract than those recorded in the free solution. This is suggesting that both extracts reduce the rate of anodic ASTM A36 mild steel dissolution in 1.5 M HCl as well as the cathodic hydrogen ion reduction [10-11]. This effect can be attributed to the blockage of active sites on the steel surface by the adsorbed film of the molecules of the studied inhibitors [11 – 13]. From the results obtained, the changes of E_{corr} are less negative than 85mV for the studied plant extracts, this suggest that both inhibitors acted as mixed type corrosion inhibitions. The polarization curves in the presence of both inhibitors show similar cathodic features as the free solution suggesting that the inhibitors do not change the mechanism of the cathodic hydrogen gas evolution associated with the corrosion process [12 – 13]. Similar observations were notices with the anodic part of the polarization curves. Values of the inhibition efficiency of the inhibitor determined from equation 1 showed that the alkaloid fraction had a stronger adsorption ability on the ASTM A36 mild steel compared to the flavonoid farction and this is in accordance with the result obtained from the thermometric analysis.

$$\%IE_i = \frac{I_{corr_b} - I_{corr_i}}{I_{corr_b}} \; x \; 100 \qquad (1)$$

Where;

IEi is the inhibition efficiency of the inhibitor, I_{corrb} is the corrosion current density of the blank and the I_{corri} is the corrosion current density of the inhibitor.

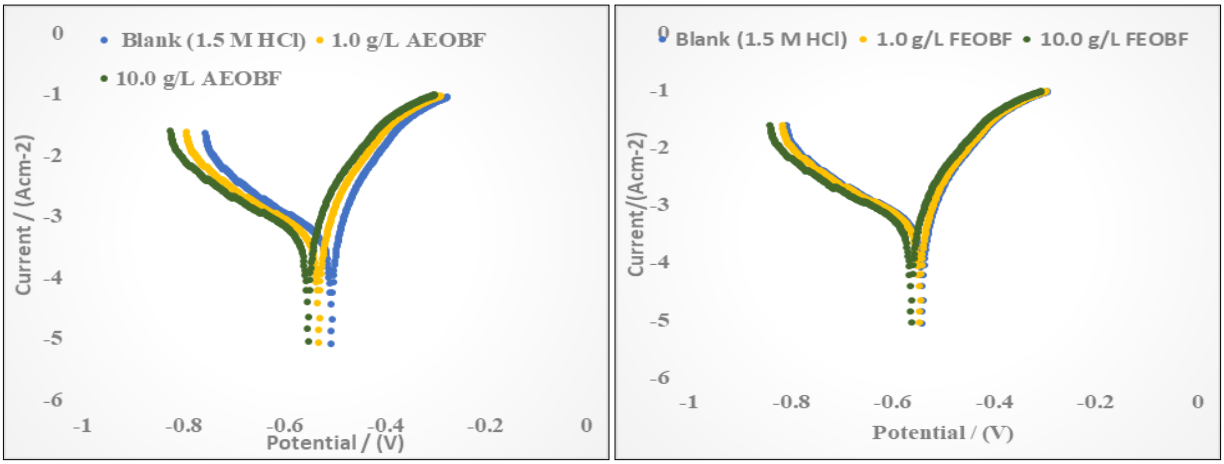

(a) **(b)**

Fig 2: Tafel plots showing effect of increasing concentrations of (a) AEOBF and (b) FEOBF on corrosion of ASTM A36 mild steel in 1.5 M HCl solutions

Table 3: *Potentiodynamic polarization parameters for* ASTM A36 mild steel in 1.5 M HCl *and with different concentrations (a) AEOBF and (b) FEOBF*

	Conc. (g/L)	Icorr (mAcm-2)	Ecorr (mV)	βc (mV/dec)	βa (mV/dec)	IEi (%)
	1.5 M HCl	1.187	-319	106	166	-
AEOBF	1.0 g/L	0.269	-271	72	124	77.3
	10 g/L	0.113	-114	39	93	90.5
	1.5 M HCl	1.187	-203	131	144	
FEOBF	1.0 g/L	0.346	-185	112	138	70.9
	10 g/L	0.206	-117	82	116	82.6

3.3 Thermodynamic consideration of metal/inhibitor interface adsorption

The enthalpy of adsorption (ΔH^*) and the entropy of adsorption (ΔS^*) for the corrosion of ASTM A36 mild steel in 1.5 M HCl *solution* was deduced from the transition state equation 2 [10 – 15].

$$log\frac{C_R}{T} = log\left(\frac{K}{Nh}\right) + \frac{\Delta S}{2.303R} - \frac{\Delta H}{2.303RT} \qquad (2)$$

Where K is the Boltzmann constant, h is the Planck constant, A is Arrhenius pre-exponential factor, T is the absolute temperature and R_c is corrosion rate. The plots and values of ΔH^* and ΔS^* obtained are given in Figures 3a – b and Table 4 respectively the positive values of ΔH^o indicate that the dissolution of the metal is an endothermic reaction [3, 12, 16]. The enthalpy values are seen to decrease with increase inhibitor concentration which indicate a physical adsorption [13, 16–18]. This is in accordance with the result of thermometric analysis that showed that inhibition was greater at lower temperatures due to lower effect of heat on the metal/inhibitor adsorption interface. The change in entropy ($\Delta S°$) was found to be greater than zero which indicates that the reaction is irreversible [15, 17, 19]. The shift towards negative values of entropy ($\Delta S°$) imply that the activated complex in the rate determining step represents association rather than dissociation, meaning that disordering is reduced [13, 17, 20-21]. The observed ΔG^*ads values (Table 5) support the mechanism of physisorption for the inhibitor's action in the acid media following the fact that ΔG^*ads values greater than -40 KJmol-1 denotes physisorptions [14, 20–25].

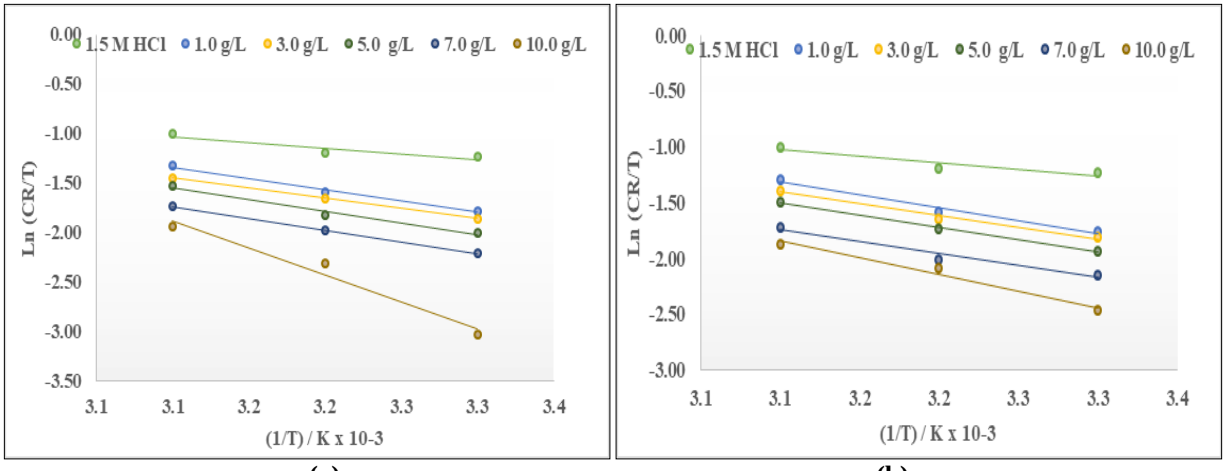

(a) **(b)**

Fig 3: Eyring transition state plots for ASTM A36 mild steel in 1.5 M HCl solution and in presence of (a) AEOBF and (b) FEOBF

In examining the effect of temperature on the corrosion inhibition process, the apparent activation energy (Ea) was calculated from the Arrhenius equation 3 through the plots in Figure 4.

$$log\frac{R_a}{R_b} = \frac{E_a}{2.303R}\left(\frac{1}{T_1} - \frac{1}{T_2}\right) \quad (3)$$

Where R_a and R_b are the corrosion rates at temperature T_1 and T_2 respectively, and R the molar gas constant. Increased activation energy (Ea) in inhibited solutions compared to blank suggest that the inhibitor is physically adsorbed on the corroding metal surface while either unchanged or lower Ea values in the presence of inhibitor suggest chemisorption [17, 21, 23 – 26]. It is observed from Table 4 that Ea values were higher in the presence of AEOBF and FEOBF in both 1.5 M HCl acid solutions compared to that in their absence leading to an increase in their corrosion rates. It has been suggested that adsorption of an organic inhibitor can affect the corrosion rate by either decreasing the available reaction area (geometric blocking effect) or by modifying the activation energy of the anodic or cathodic reactions occurring in the inhibitor-free surface in the course of the inhibited corrosion process [11, 22, 27-30]. The Ea values support the earlier proposed physisorption mechanism.

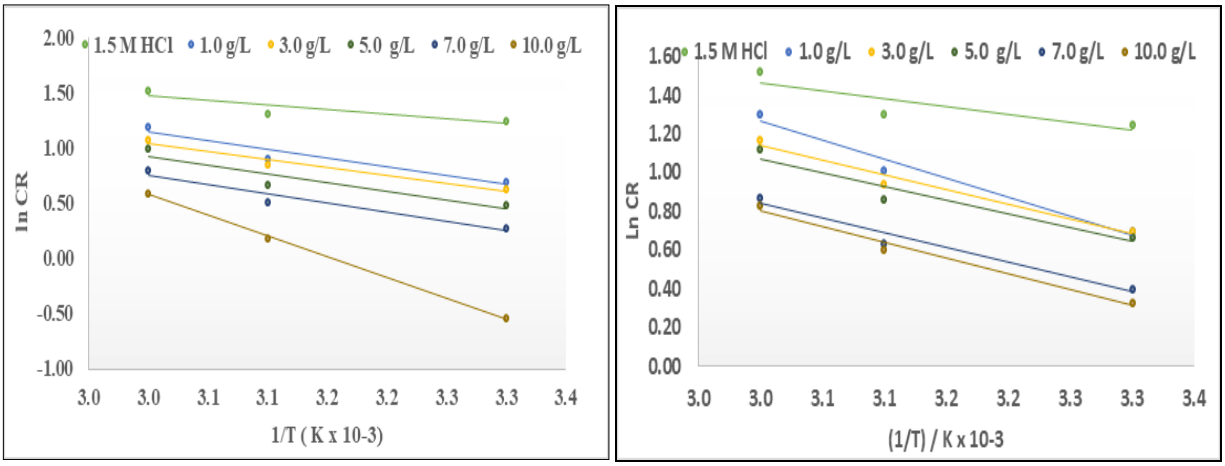

(a) **(b)**

Fig 4: Arrhenius plots for ASTM A36 mild steel in 1.5 M HCl solutions and in the presence of (a) AEOBF and (b) FEOBF

Table 4: Thermodynamic parameters for ASTM A36 mild steel in 1.5 M HCl solution and in the presence of (a) AEOBF and (b) FEOBF

	AEOBF			FEOBF		
Conc. (g/L)	Ea	ΔHads kJ/mol	ΔSads kJ/mol	Ea	ΔHads kJ/mol	ΔSads kJ/mol
1.5 M HCl	10.15	26.12	-273.05	10.15	26.12	-273.05
1.0 g/L	17.01	21.03	-222.15	15.24	20.13	-213.15
3.0 g/L	17.62	19.11	-202.95	15.68	17.07	-182.55
5.0 g/L	18.19	17.92	-191.05	16.52	16.51	-176.95
7.0 g/L	18.59	12.49	-136.75	17.07	15.87	-170.55
10.0 g/L	19.11	8.72	-99.05	18.11	11.69	-128.75

3.4 Langmuir adsorption isotherm description

The surface coverage (θ) values for different concentrations of AEOBF and FEOBF in 1.5 M HCl acid solution were evaluated from the thermometric analysis data. The data were tested graphically to find a suitable adsorption isotherm to describe the adsorption characteristics of the inhibitors [31 – 37]. The Langmuir isotherm may be formulated as equation 4

$$\frac{c}{\theta} = \frac{1}{k} + c \quad (4)$$

Where *c* is the inhibitor concentration and *k* equals the equilibrium constant for the adsorption/desorption process. A plot of Log (Θ/C) against Log C (Fig. 5) showing a straight line with regression values R>= 0.99 indicate that adsorption is monolayer with respect to Langmuir isotherm [1, 9, 24, 33, 38 – 40]. It is also observed that although these plots are linear, the gradients are never unity, contrary to what is expected for ideal Langmuir adsorption isotherm equation. Organic molecules having polar atoms or groups which are adsorbed on the metal surface may interact by mutual repulsion or attraction and this may be advocated as the reason for the departure of the slope values from unity [13, 21, 33, 41 – 44]. The calculated ΔG*ads values are listed in Table 5. The negative values of adsorption free energy indicate that the adsorption of the inhibitor molecules is a spontaneous process and the inhibitor is very stable on the surface [6, 9, 37, 45 – 48]. The standard adsorption free energy ΔG_{ads} values (shown in Table 5) were obtained using the equation 5:

$$k = \frac{1}{55.5}\exp\frac{-\Delta G_{ads}}{RT}$$

Where R is the gas constant, T is the temperature, and 55.5 is the molar concentration of water in aqueous solution. Values of standard free energy of adsorption, ΔG_{ads} were obtained from the reciprocal of the intercept of Fig. 5. The constant k is related to standard free energy of adsorption by the equation 5 [15, 19, 22, 39, 48 – 50]. The observed ΔG_{ads} values (Table 5) support the mechanism of physisorption for the inhibitor's action in acid media.

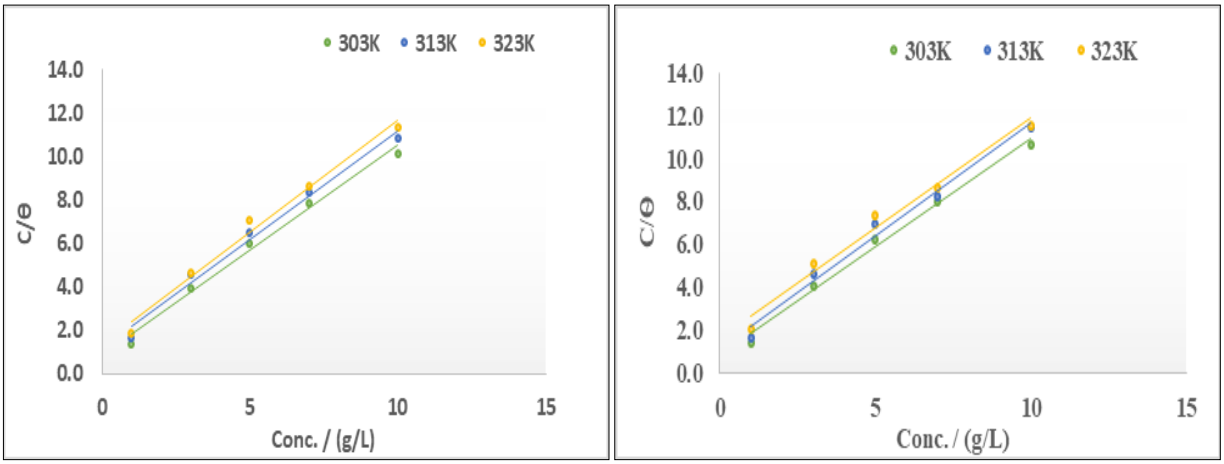

Fig 5: Langmuir adsorption isotherm for ASTM A36 mild steel in 1.5 M HCl solution and in the presence of (a) AEOBF and (b) FEOBF

Table 5: Adsorption parameters for ASTM A36 mild steel in 1.5 M HCl containing (a) AEOBF and (b) FEOBF

	AEOBF				FEOBF			
Temp. (K)	k (g/L)	R^2	Slope	$-\Delta G^*_{ads}$ (kJ/mol)	k (g/L)	R^2	Slope	$-\Delta G^*_{ads}$ (kJ/mol)
303	0.726	0.986	1.027	93.11	0.607	0.980	1.022	88.60
313	0.830	0.986	0.996	99.67	0.862	0.985	1.048	100.65
323	1.181	0.989	0.967	112.32	1.176	0.991	1.006	112.21

4. Conclusion

The following conclusion was drawn from the research:

1. Alkaloid and flavonoid synthesised inhibitors of *Oenothera biennis* (Common evening primrose) flowers showed very efficient inhibitive action on ASTM A36 mild steel in 1.5 M HCl acid solution with inhibition efficiency of 97.6, 90.1 and 80.2% for alkaloid and 91.4, 83.5 and 76.8% for flavonoid at 303, 313 and 323 K.
2. Decreasing values of corrosion current density was observed with increasing inhibitor concentration indicating that the inhibitors were strongly adsorbed on the metal surface with less desorption on agitation.
3. Mechanism of adsorption was found to be physical adsorption mechanism and the adsorption process was monolayer an indication that the inhibitors were apparently best at lower temperatures.
4. The inhibitors were also found to be very stabled, associative and spontaneous which allows for a better adsorption not only at lower temperatures but at moderately higher temperatures as well.

The thermodynamic parameters, along with the kinetic parameters, showed that the adsorption of *Oenothera biennis* molecules onto ASTM A36 steel obeyed the Langmuir isotherm model, and the adsorption at metal–electrolyte interfaces involved predominantly physisorption mechanism.

5. References

1. Nnanna, LA, Uchendu KO, Nwosu FO, Ihekoronye U, Eti PE. Gmelina arborea bark extracts as corrosion inhibitor for mild steel in an acidic environment. Int. J Mater. Chem. 2014; 4(2):34-39.
2. Li X, Deng S, Fu H. Inhibition of the corrosion of steel in HCl, H2SO4 solutions by bamboo leaf extract, Corros. Sci. 2014; 62:163-175.
3. El Hamdani N, Fdil R, Tourabi M, Jama C, Bentis F. Alkaloids extract of Retama monosperma (L.) Boiss. Seeds used as novel eco-friendly inhibitor for carbon steel corrosion in 1 M HCl solution: Electrochemical and surface studies. Appl. Surf. Sci. 2015; 357:1294-1305.
4. AZoM. ASTM A36 Mild/Low Carbon Steel. https://www.azom.com/article.aspx?ArticleID=6117. 2012; Pp. 3
5. Jill Mallory MD. Integrative medicine. 4th Ed, 2018, 535-541.
6. Eddy NO, Momoh Yahaya H, Oguzie EE. Theoretical and experimental studies on the corrosion inhibition potentials of some purines for aluminum in 0.1 M HCl. Journal of Advance Research. 2015; 6(2):203-217.
7. Ikpi ME, Abeng FE. Electrochemical impedance spectroscopy and gravimetric study of the corrosion inhibition of API 5L X-52 steel in HCl medium by Levofloxacin. Intl. J Sci. Research. 2017; 6(6):6230-628.
8. Jothi, RV, Maheshwari P, Saratha R, Vadivu DS. A study on inhibitive action of Bauhinia racemose Lam. Extract as green corrosion inhibitor for mild steel in HCL medium" Asian journal of research in chemistry. 2017; 10(5):611-615
9. Abd El Lateef HM, Soliman KA, Tantawy AH. Novel synthesized Schiff Base-based cationic gemini surfactants: Electrochemical investigation, theoretical modeling and applicability as biodegradable inhibitors for mild steel against acidic corrosion. J Mol. Liq. 2017; 232:478-498.
10. Deng S, Li X. Inhibition by *Jasminum nidiflorum lindl.* Leaves extract of the corrosion of aluminium in HCl solution. Corros Sci. 2012; 62:407-415.
11. Cookey GA, Tambari BL, Iboroma DS. "Evaluation of corrosion inhibition potentials of green tip forest lily (Clivia nobilis) leaves extract on mild steel in acid media". Journal of applied sci. Env.Mgt. 2018; 22(1):90-94.
12. Feng F, Yin C, Zhang H, Li Y, Song X, Chen Q. Cationic Gemini surfactants with a bipyridyl spacer as

corrosion inhibitors for carbon steel. ACS Omega. 2018; 3:18990-18999.
13. Dagdag O, Harfi AE, Cherkaoui O, Safi Z, Wazzan N, Guo L, *et al*. Rheological, electrochemical, surface, DFT and molecular dynamics simulation studies on the anticorrosive properties of new epoxy monomer compound for steel in 1 M HCl solution. RSC Adv. 2019; 9:4454-4462.
14. Ugi BU, Obeten ME, Uwah IE, Okafor PC. Aluminium corrosion abatement using non toxic and eco – friendly organic inhibitors. Journal of Global Ecology and Environment. 2016; 4(4):242-252.
15. Srivastava M, Tiwari P, Srivastava SK, Kumar A, Ji G, Prakash R. Low cost aqueous extract of Pisum sativum peels for inhibition of mild steel corrosion, J. Mol. Liq. 2018; 25(4):368.
16. Saxena A, Prasad D, Haldhar R, Singh G, Kumar A. Use of Saraca ashoka extract as green corrosion inhibitor for mild steel in 0.5 M H2SO4, J. Mol. Liq. 2018; 25(8):97.
17. Alvarez PE, Fiori Bimbi MV, Neske A, Brandán SA, Gervasi CA. Rollinia occidentalis extract as green corrosion inhibitor for carbon steel in HCl solution, J. Ind. Eng. Chem. 2018; 58:99.
18. Hui C, Zhenghao F, Jinling S, Wenyan S, Qi X. Corrosion inhibition of mild steel by Aloes extract in HCl solution medium. Int. J electrochem. Sci. 2013; 8:734.
19. Louis H, Japari J, Sadia A, Philip M, Bamanga A. Photochemical screening and corrosion inhibition of Poupartia birrea back extract as a potential green inhibitor for mild steel in 0.5 M H2SO4 solution, World News Nat. Sci. 2017; 10:100.
20. Tawfik SM, Abd Elaal AA, Aiad I. Three gemini cationic surfactants as biodegradable corrosion inhibitors for carbon steel in HCl solution. Res. Chem. Intermed. 2016; 42:1101-1123.
21. Sin HLY, Rahim AA, Gan CY, Saad B, Salleh, M. Umeda MI. Aquilaria subintergra leaves extracts as sustainable mild steel corrosion inhibitors in HCl, Measurement. 2017; 109:345.
22. Okewale AO, Olaitan A. The use of rubber leaf extract as a corrosion inhibitor for mild steel in acidic solution, Int. J. Mater. Chem. 2017; 7:13.
23. Mobin M, Aslam R, Aslam J. Nontoxic biodegradable cationic gemini surfactants as novel corrosion inhibitor for mild steel in hydrochloric acid medium and synergistic effect of sodium salicylate: Experimental and theoretical approach. Mater. Chem. Phys. 2017; 191:151-167.
24. Ugi BU, Abeng FE, Obeten ME, Uwah IE. Management of aqueous corrosion of federated mild steel (Local constructional steel) at elevated temperatures employing environmentally friendly inhibitors: Matricaria chamomilla plant. Intl. J Chem. Sci. 2019; 3(1):6-12.
25. Olesegun SJ, Okoronkwo EA, Okotete AE, Ajayi OA. Gravimetric and electrochemical studies of corrosion inhibition potential of acid and ethanol extract of siam weed on mild steel, Leonardo J Sci. 2016; 9:42.
26. Goyal M, Kumar S, Bahadur I, Verma C, Ebenso EE. Organic corrosion inhibitors for industrial cleaning of ferrous and nonferrous metals in acidic solutions. A review. J Mol. Liq, 2018; 256:565-573.
27. Sin HLY, Rahim AA, Gan CY, Saad B, Salleh, M. Umeda MI. Aquilaria subintergra leaves extracts as sustainable mild steel corrosion inhibitors in HCl, Measurement. 2017; 109:345.
28. Chidiebere MA, Oguzie EE, Liu L, Li Y, Wang Y. Adsorption and corrosion inhibiting effect of riboflavin on Q235 mild steel corrosion in acidic environments. Mater. Chem. Phys. 2015; 156:104.
29. Krishnegowda PM, Venkatesha VT, Krishnegowda PKM, Shivayogiraju SB. Acalypha torta leaf extract as green corrosion inhibitor for mild steel in hydrochloric acid solution. Ind. Eng. Chem. Res 2013; 52(2):722-728.
30. Abeng FE, Ikpi ME, Uwakwe K, Ikpi G. Corrosion inhibition and adsorption characteristics of API 5L X – 52 steel by an antibiotic drug in HCl solution. Intl. Resear. J. Pure Appl. Chem. 2017; 15(3):1-12.
31. Fitoz A, Nazır H, Özgür, Emregül E, Emregul K. An experimental and theoretical approach towards understanding the inhibitive behavior of a nitrile substituted coumarin compound as an effective acidic media inhibitor. Corros. Sci., 2018; 133: 451-464.
32. Hassannejad H, Nouri A. Sunflower seed hull extract as a novel green corrosion inhibitor for mild steel in HCl solution, J. Mol. Liq. 2018; 25(4):382.
33. Qiang Y, Zhang S, Tan S, Chen S. Evaluation of Ginkgo leaf extract as an eco-friendly corrosion inhibitor of X70 steel in HCl solution, Corros. Sci. 2018; 133:16.
34. Mohammed NR, Fadwa MA, Atega MA Corrosion inhibition of 316 stainless steel in 20% (W/W) HCl solution using Dithizone. American journal of Applied Chemistry. 2014: 2(1): 1
35. Faustin M, Maciuk A, Salvin P, Roos C, Lebrini M. Corrosion inhibition of C38 steel by alkaloids extract of Geissospermum laeve in 1M hydrochloric acid: Electrochemical and phytochemical studies. Corros. Sci., 2015; 92:287-300.
36. Ugi BU, Obeten ME. Inhibitory impact of crude phytochemical compounds of *Symphytum officinali* (Comfrey) leaves on the corrosion of copper by Hydrogen tetraoxosulphate (IV) (H_2SO_4) acid solution. SSRG International Journal of Applied Chemistry. 2018; 5(2):22.
37. Kumar S, Vashisht H, Olasunkanmi LO, Bahadur I, Verma H, Goyal M, *et al*. Polyurethane Based Triblock Copolymers as Corrosion Inhibitors for Mild Steel in 0.5MH2SO4. Ind. Eng. Chem. Res. 2017; 56:441-456.
38. Odewunmi NA Umoren SA, Gasem ZM. Watermelon waste products as green corrosion inhibitors for mild steel in HCl solution. J. Environ. Chem. Eng. 2015; 3:286-296.
39. Kaczerewska O, Leiva Garcia R, Akid R, Brycki B, Kowalczyk I, Pospieszny T. Effectiveness of O-bridged cationic gemini surfactants as corrosion inhibitors for stainless steel in 3MHCl: Experimental and theoretical studies. J. Mol. Liq. 2018; 249:1113-1124.
40. Loto RT, Loto CA. Anticorrosion properties of the symbiotic effects of Rosmarinus officinalis and trypsin complex on medium carbon steel. Result in Physics. 2018; 10:99-106.
41. Okafor PC, Apebende EA. Corrosion inhibition

characteristics of Thymus vulgaris, Xylopia aethiopica and Zingiber officinale extracts on mild steel in H2SO4 solution" Pigment & Resin Tech. 2014; 43(6):357-364.
42. Marzorati S, Verotta L, Trasatti SP. Green corrosion inhibitors from natural sources and biomass wastes. Molecules. 2019; 24:48.
43. Popoola LT. Progress on pharmaceutical drugs, plant extracts and ionic liquids as corrosion inhibitors. Heliyon. 2019; 5(2):e01143.
44. Kesavan D, Gopiraman M, Sulochana N. Green Inhibitors for Corrosion of Metals: A Review. Che Sci Rev Lett. 2012; 1(1):1-8.
45. Alobaidy AH, Kadhum A, AlBaghdadi SB, AlAmiery AA, Kadhum AAH, yousif E, *et al*. Eco-Friendly Corrosion Inhibitor: Experimental Studies on the Corrosion Inhibition Performance of Creatinine for Mild Steel in HCl Complemented with Quantum Chemical Calculations. Int. J Electrochem. Sci. 2015; 10:3961-3972.
46. Jwad H, Rifaat HH, Abdul ML, Kadhuma MD, Al Amieryd AH, AA Gaaz TS. Development of new corrosion inhibitor tested on mild steel supported by electrochemical study. Results in Physics. 2018; 8:260-1267.
47. Odusote JK, Ajayi OM. Corrosion Inhibition of Mild Steel in Acidic Medium by Jath-ropha Curcas Leaves Extract. Journal of Electrochemical Science and Technology. 2013; 4(2):81-87.
48. Alibakhshi E, Ramezanzadeh M, Bahlakeh G, Ramezanzadeh B, Mahdavian M, Motamedi M. Glycyrrhiza glabra leaves extract as a green corrosion inhibitor for mild steel in 1 M hydrochloric acid solution: Experimental, molecular dynamics, Monte Carlo and quantum mechanics study. J Mol. Liq. 2018; 255:198.
49. Odusote JK, Owalude DO, Olusegun SJ, Yahya RA. Inhibition efficiency of Moringa oleifera leaf extract on the corrosion of reinforced steel bar in HCl solution" The west indian journal of engineering, 2016; 38(2): 64-70.
50. Ituen E, Akaranta O, James A, Sun S. Green and sustainable local biomaterials for oilfield chemicals: Griffonia simplicifolia extract as steel corrosion inhibitor in hydrochloric acid, Sustain, Mater. Technol. 2017; 11:18-33.